Current Topics in Analytical Chemistry
Vol. 14, 2022

Original Article

Pulsed-flow analysis and internet-of-things as tools for environmental analytical chemistry: An automated on-site analyzer for phosphorus in water bodies

Moisés Knochen*, Guillermo Roth and Pablo González

Universidad de la República, Faculty of Chemistry, Group for Instrumentation and Automation in Analytical Chemistry (GIAQA), Av. Gral. Flores 2124, 11800 Montevideo, Uruguay.

ABSTRACT

This paper describes the design, construction, and evaluation of a simple, battery-operated automated analyzer for on-site determination of reactive soluble phosphorus in polluted water bodies. The analyzer is based on pulsed-flow analysis, implemented with just two solenoid micropumps. Phosphorus is detected using the molybdovanadate photometric method for orthophosphate; detection employing an UV LED is used for increased sensitivity. The whole system is controlled by an ATMega328 microcontroller, including the operation of the flow system, measurement of the absorbance and data processing. Analytical results, as well as other relevant data are sent *via* wireless internet to a cloud-based internet-of-things (IoT) server, where they can be monitored and retrieved for later processing. Analytical figures of merit were evaluated. Linearity was verified up to a concentration of 6 mg-P L^{-1} (R^2 = 0.996). Precision (s_R (%), n = 8) was in the range of 3%-12% for water samples with phosphorus contents in the 1–5 mg-P L^{-1} range. When compared with a reference method, accuracy of the results for those samples (average, n = 8) ranged from 96.2% to 105.8%. Based on these results, its simplicity and low cost, the analyzer was deemed fit for the purpose. The use of cloud storage and IoT technologies provided additional benefits in terms of data availability away from the sampling point.

*Corresponding author: mknochen@fq.edu.uy

KEYWORDS: phosphorus, on-site, automated analyzer, pulsed-flow analysis, internet-of-things.

INTRODUCTION

The determination of phosphorus in water bodies has received attention for decades. The interest in these analyses stems from the increasing evidence of the harmful effect of high phosphorus concentrations in water bodies, due to its role as a nutrient. High levels of one or several nutrients, combined with certain conditions of ambient light and temperature facilitate a rapid growth of some components of phytoplankton. This in turn may lead to undesirable consequences such as anoxia of the water body, or the production of toxic metabolites by some of the bacterial species. One well known example of the latter is the phenomenon known as “algal blooms”, where different species of cyanobacteria (“blue-green algae”) experience an explosive growth, with some of those species producing metabolites known as cyanotoxins, which are toxic for humans and animals [1].

One of the most important anthropogenic sources of phosphorus in water are phosphate fertilizers used in farming since the fraction not absorbed by the soil and plants is transported to rivers and lakes by runoffs. Also of concern are improperly managed industrial effluents. Thus, high phosphorus levels (even in the mg L^{-1} range) are often found in water bodies such as rivers and lakes in connection to agricultural or industrial activities.

For this reason, national regulatory bodies establish limits to the acceptable concentrations of phosphorus in surface water. These limits are very low, in the μg L^{-1} level, which presents a challenge for analytical methods. The maximum allowable concentration of phosphorus in industrial effluents has also been established by regulatory bodies, and usually lies in the mg L^{-1} range. It is clear that analytical chemistry has an outstanding role as the provider of reliable information for decision making.

The determination of phosphorus in water bodies and effluents in the μg L^{-1} – mg L^{-1} range can be carried out by several methods based on techniques such as UV-Visible spectrophotometry, ion chromatography, etc. [2]. Flow analysis techniques are often employed for the automation of this determination in the laboratory but also for on-site measurements [3-6].

For the monitoring of phosphorus and other nutrients in water bodies and effluents, the current trend is to resort to automated on-site analyzers [7-9]. These feature several advantages, such as independence from human labor, faster availability of results and internet connectivity, enabling decisions to be made at places distant from the sampling site. The widespread availability of low-cost electronics, wireless internet and cloud-based storage and data handling (in some cases free of charge), have favored the explosive growth of sensors and automated devices connected to the internet, collectively known as the internet-of-things (IoT) [10]. Together these resources constitute a formidable tool which can be taken advantage of to produce useful analytical information [11, 12].

On-site automated analyzers are usually based on flow analysis techniques, employing a selective chemical reaction followed by optical detection. The two chemistries most frequently employed for the determination of phosphorus as orthophosphate are those of reduced molybdophosphate ("molybdenum blue") [5, 13] and molybdovanadate [14, 15]. For laboratory methods, the former is usually preferred due to better sensitivity; however, the reagents employed, including reductants such as ascorbic acid or stannous chloride, are not stable enough for long-term field use. The complex chemistry behind the different reactions involved has been discussed in detail in a comprehensive review [16]. The molybdovanadate method, on the other hand, presents several advantages, such as better reagent stability, less chemical interferences, and a simpler reagent. When compendial methods (such as APHA 4500-P C [17]) are followed, it is customary to measure at wavelengths in the range 400 – 490 nm, situated on a side of the absorption band. The low absorptivities at those wavelengths are the main reason behind the poor sensitivity frequently associated to this method. However, sensitivity can be enhanced significantly by measuring at a wavelength closer to the maximum of the absorption band, which is located at around 315 nm [18].

Concerning the automation of the analytical determinations, previous work [19, 20] has shown the utility of pulsed-flow analysis for the determination of nutrients in environmental studies. Pulsed-flow analysis [21-23] is a branch of flow analysis where individual solenoid micropumps are used as propelling element for each liquid stream. Analytical systems so designed are compact and robust. One of the advantages found is that solenoid micropumps generate a positive pressure surge followed by a small period of negative pressure, hence mixing is enhanced. Multi-pumping pulsed-flow systems share some of the advantages of multicommutated flow analysis systems, one of them being the possibility of implementing binary sampling [24], which is another strategy for enhancing the mixing of the fluids. Also, the use of independent pumps for each channel adds flexibility for the system. These systems require computer control, which can be carried out for instance by means of cheap microcontroller platforms. Internet access can be easily added to such systems transforming them into powerful tools for data generation and storage.

This paper describes the design, construction, and evaluation of a simple automated on-site analyzer for the determination of dissolved reactive phosphorus at the parts-per-million range in polluted water bodies. The analyzer is based on the molybdovanadate reaction employing pulsed flow analysis with photometric detection. Standard off-the-shelf electronics was used throughout to keep costs at a minimum. It features remote-reporting capabilities by means of wireless internet, employing a free cloud-based storage and reporting platform.

MATERIALS AND METHODS

Reagents

All reagents were of analytical reagent grade. Ultrapure deionized (DI) water (ISO grade I) was produced in a Millipore DirectQ-5 purifier.

Reagent for the automated system was prepared by dissolving in enough water 1.785 g of ammonium molybdate tetrahydrate and 0.0895 g of ammonium metavanadate, then adding 23.75 mL of concentrated hydrochloric acid and adding water up to 250 mL and stirring until solids were totally dissolved.

Standard phosphorus solutions were prepared by dissolving 219.5 mg anhydrous dihydrogen potassium phosphate in DI water and diluting to 1000 mL; this concentrated standard solution was daily diluted with DI water as necessary to obtain standards suitable for calibration of the system.

Analytical system

The analytical system is depicted in Figure 1. It is composed by the sampling and pulsed-flow subsystems. The sampling subsystem involves the intake coarse filter and tubing, a 12-V peristaltic mini pump, a 25-mm filter holder with 1.2 µm glass-microfiber filter (Whatman GF/C), and a 50-mL intermediate reservoir, whose purpose is to ensure that a sufficient volume of representative sample will be available to the pulsed-flow subsystem prior to the beginning of each analytical cycle.

The pulsed-flow subsystem is made up of two 12-V solenoid micro pumps (Cole Parmer 73120-10, 20-µL stroke), three 12-V solenoid valves (part of a four-valve manifold, NResearch 225T071), a 100-cm long mixing coil, and a 10-mm, 80-µL quartz flow cell (Starna). The mixing coil and all connections were made of 0.8 mm (internal diameter) FEP tubing. The 100-cm long mixing coil is coiled in “8” shape.

The detection system is composed of a 365-nm LED with focusing lens (Nichia, NSHU591B) and a UV photodiode (Roithner Lasertechnik, EPD-440-011), placed at each side of the flow-cell holder. The signal from the photodiode is fed to an operational amplifier (TL081) configured in the transimpedance mode. The output of the amplifier is in turn connected to one of the analog inputs of a ADS1115 16-bit analog-to-digital converter (ADC) board.

The LED was fed by a LM334 constant-current generator integrated circuit, connected to the +12-V rail. The current supplied to the LED was

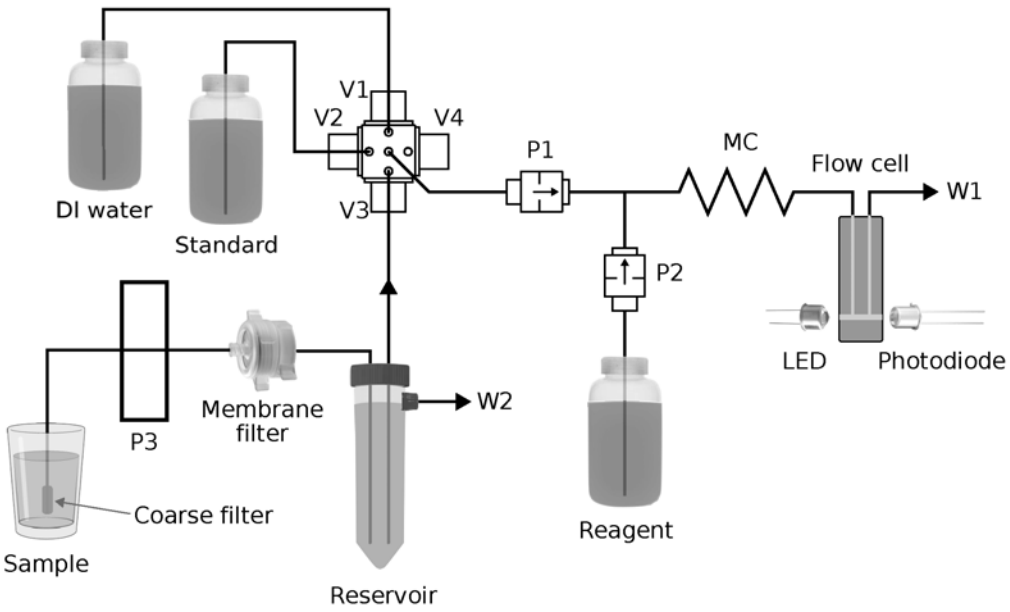

Figure 1. Diagram of the flow system. P1, P2: solenoid micropumps. P3: peristaltic minipump. V1, V2, V3, V4: solenoid valves (V4 unused). MC: mixing coil. W1: waste vessel. W2: sample overflow.

adjusted in such a way that with the flow cell filled with DI water the output of the operational amplifier was around 4 V.

System control

The whole system was controlled by an Arduino Nano board with an ATMega328 microcontroller unit (MCU). Solenoid micro pumps, solenoid valves, the peristaltic minipump and the LED are controlled from several input/output (I/O) digital ports of the MCU via a ULN2803 Darlington driver. For the operation of the solenoid valves, pulse-width modulation (PWM) was used to apply the appropriate holding power as recommended by the manufacturer; the same technique was used to set the required speed of the peristaltic mini pump.

Data acquisition from the photometric detection was carried out by the ADS1115 ADC, which communicates with the MCU *via* the I^2C serial bus.

Temperature within the box containing the electronics was measured by a DS18B20 digital temperature sensor (Maxim), which communicates with the MCU *via* the 1-Wire® serial bus.

The power supply of the system consisted of a 12000-mAh power bank featuring a 12-V output. 5 V for the MCU was obtained by means of a switching DC-DC module. Negative supply (-12 V) for the operational amplifier was provided by an ICL7662 module (Maxim).

The voltage of the +12 V output of the power bank was measured periodically using an analog input of the MCU.

The block diagram of the electronic circuitry is depicted in Figure 2.

Communications and cloud storage

Communications were provided by a SIM800EVB GSM/GPRS modem operating under control of the MCU. In this way the system can communicate *via* wireless internet at any site where GSM is available.

Data were sent to an IoT cloud platform (ThingSpeak, www.thingspeak.com) which can be used free of charge for low-traffic applications. Data sent include output voltage from the operational amplifier during photometric adjustment, absorbances for blank, standard, and sample, calibration slope, sample concentration, internal temperature, and voltage of the power bank. Some of these were used for monitoring and diagnosing the analyzer itself.

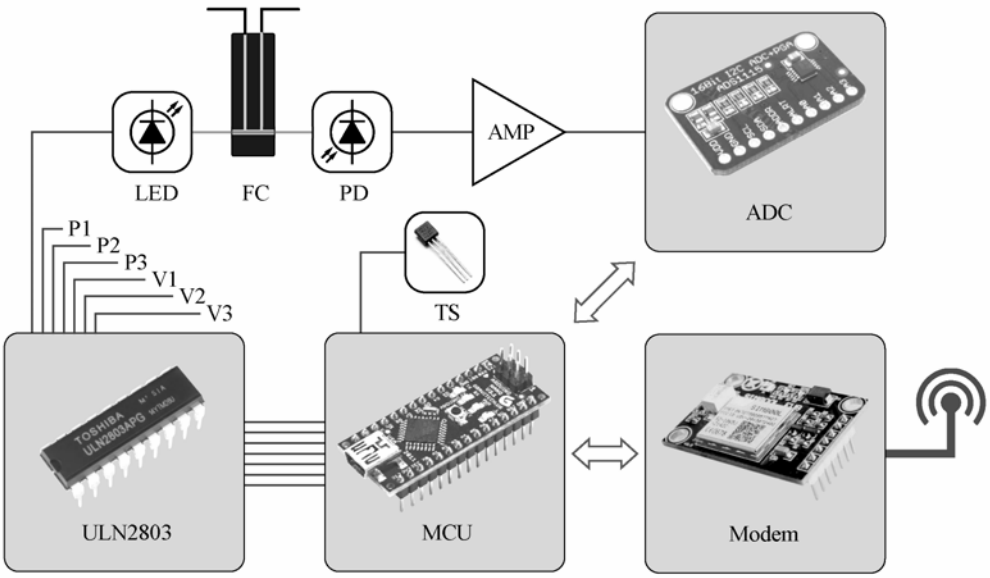

Figure 2. Block diagram of the electronic circuit. LED: light-emitting diode. FC: flow cell. PD: photodiode. AMP: operational amplifier. ADC: analog-to-digital converter. ULN2803: Darlington driver. MCU: microcontroller unit. P1, P2: solenoid micropumps. P3: peristaltic minipump. V1, V2, V3: solenoid valves. TS: DS18B20 temperature sensor

Construction

The whole analyzer was housed in a fiberglass-reinforced polyester IP-65 cabinet (dimensions 40 x 30 x 21 cm) fitted with a hinged door. The electronic components were in turn housed in two independent watertight boxes within the cabinet.

The holder for the flow cell and other auxiliary parts were built by 3D-printing employing a Qidi Tech X-One 3D printer and PLA filament.

Deionized water, reagent, and phosphorus standard were stored in low density polyethylene bottles (500-, 500- and 100-mL capacity respectively). A 1000-mL polyethylene bottle was used to receive the waste.

Operation of the system

Firmware for the Arduino Nano MCU was programmed in Arduino language (based on C++) by means of the Arduino Integrated Development Environment (IDE). The firmware controls the whole operation of the system including sampling, analysis, calculation, and communications.

The first-time routine begins with purging and filling all lines by pumping the corresponding fluid (deionized water, standard solution, reagent, and sample) for 20 seconds to displace air and other previous contents of the system.

The rest of the working cycle is described in Table 1.

First, the voltage of the power bank is measured to decide whether operation is possible. Then, with the LED turned off, the dark signal S_0 is measured and stored. Then the LED is turned on, the flow cell filled with DI water, and the reference signal S_{Ref} measured and stored. In this way the photometric scale is defined. Following this, all absorbances can be calculated as $A = -\log_{10} ((S_x - S_0) / (S_{Ref} - S_0))$

During each analytical cycle, the activation of valves V1, V2 and V3 allows the selection of DI water, standard solution, or sample to be pumped for measurement. Color forming reaction and absorbance measurement are carried out first with DI water (V1 activated) obtaining the blank measurement, and then with standard solution (V2 activated), allowing the calculation of a linear calibration curve. The next step is turning the peristaltic mini pump on during 250 seconds in order to replace the previous content of the intermediate reservoir with fresh sample. Then the sample is subject to color development. For this purpose, P1 and P2 are alternatively activated for 150 ms and released for 350 ms, thus inserting in the flow system a stack consisting of 10 segments of sample (or standard or water, depending on the valve activated) and 10 segments of reagent in interleaved fashion (Figure 3). In this way binary sampling is implemented allowing a better mixture to be obtained [24]. Thus, 200 µL of

Table 1. Working cycle of the analyzer.

Step	Action	Description
1	Level of battery charge	The current voltage of the power bank is measured; if less than 10 V, the analyzer goes into sleep mode
2	Photometric adjustment	0% and 100% transmittance signals are measured
3	Measurement of reagent blank	Absorbance of the reagent blank is measured in triplicate
4	Measurement of calibration standard	Absorbance of the calibration standard is measured in triplicate
5	Calibration	The parameters of the linear calibration equation are obtained and saved in the memory of the Arduino board
6	Sample renewal	Peristaltic pump is activated to clean and fill the sample reservoir
7	Measurement of sample blank	Absorbance of the sample (without being mixed with the reagent) is measured
8	Measurement of sample	Absorbance of the sample is measured in triplicate. Phosphorus concentration is calculated
9	Measurement of temperature	The temperature inside the analyzer is measured
10	Send data to cloud	The data obtained is sent to the external server

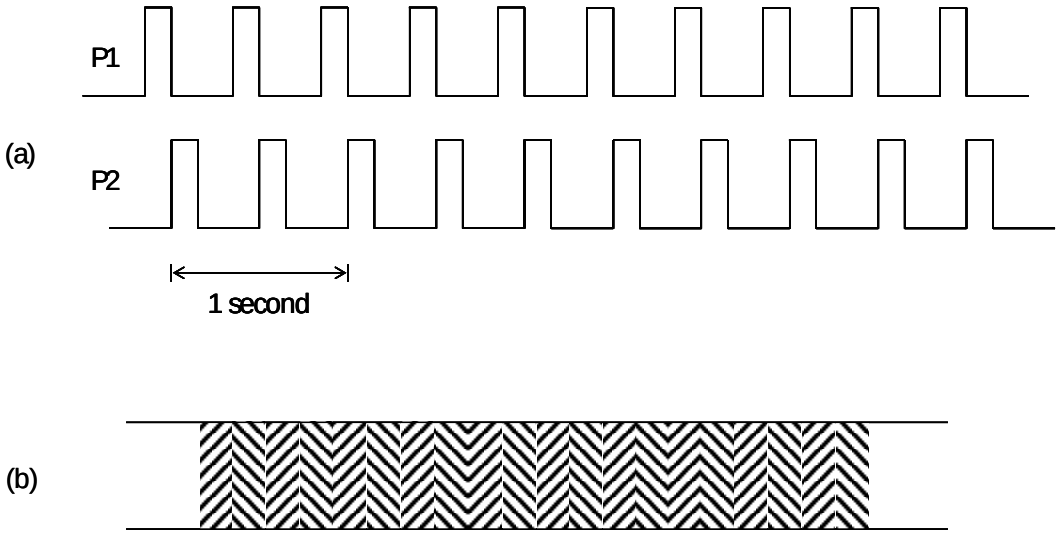

Figure 3. (a) Activation pattern of pumps P1 (sample/standard/blank) and P2 (reagent) for color-forming reaction. (b) Representation of the stack of sample (///) and reagent (\\\) segments formed through binary sampling

sample and 200 µL of reagent are inserted and mixed while travelling through the mixing coil. The bolus so obtained is then transported to the detection flow cell by a stream of pulses of DI water; the number of pulses was adjusted to ensure that the bolus reaches the flow cell and continues to waste.

For each measurement (i.e. sample, standard, or blank), the transient signal obtained (absorbance versus time) is processed by the firmware in order to assess the baseline and the absorbance at the apex. The baseline-corrected peak-height (absorbance) is calculated and stored in memory within the MCU. This allows calculation of the calibration slope and then of the concentration of the analyte in the sample.

Given that the measurements can be carried out in duplicate or triplicate, the firmware then calculates the average result.

Once the analytical cycle has finished, the system establishes communication with the IoT platform *via* the modem, and data, including temperature and voltage are sent for storage and later retrieval.

Afterwards the LED and the valves are turned off and the MCU goes into a “deep sleep” mode for a specified period in order to decrease power consumption.

Reference method

For the estimation of the accuracy of results, samples were analyzed by the APHA manual method based on the same chemistry [17].

RESULTS AND DISCUSSION

Flow system

Given the flexibility provided using individual solenoid micropumps, several designs are possible to attain the desired purpose. In the first stages of the project, three individual micropumps were used for reagent, blank and sample or standard (these two being selected by means of a solenoid valve), with the three streams converging into the inlet of the mixing coil.

However, when testing the performance of this system, it was soon noticed that the results were biased, and hence accuracy was affected. Further investigation led to the fact that the between-pump variability in the average volume delivered could be as much as 20%, resulting in inaccurate calibrations due to different volumes being delivered for standard and sample. In previous works of this group this problem was not detected, probably due to the use of micropumps having very close specifications.

However, having to choose the micropumps by hand was not an option. Thus, a new flow system

Table 2. Activation scheme for the measurement of the standard solution.

Step	Action	Description
1	V1 on	Carrier stream is selected
2	P1 is pulsed 10 times	200 μL of DI water is pumped
3	V1 off, V2 on	Standard solution stream is selected
4	P1 is pulsed 10 times	200 μL of standard solution is pumped, filling the tubing section up to the junction point of P1 and P2
5	P1 and P2 are pulsed 10 times each in interspersed fashion	Standard solution and reagent are inserted as shown in Figure 4
6	V2 off, V1 on	Carrier stream is selected
7	P1 is pulsed 60 times	1200 μL of DI water is pumped; the bolus is transported to the flow cell and the analytical signal recorded

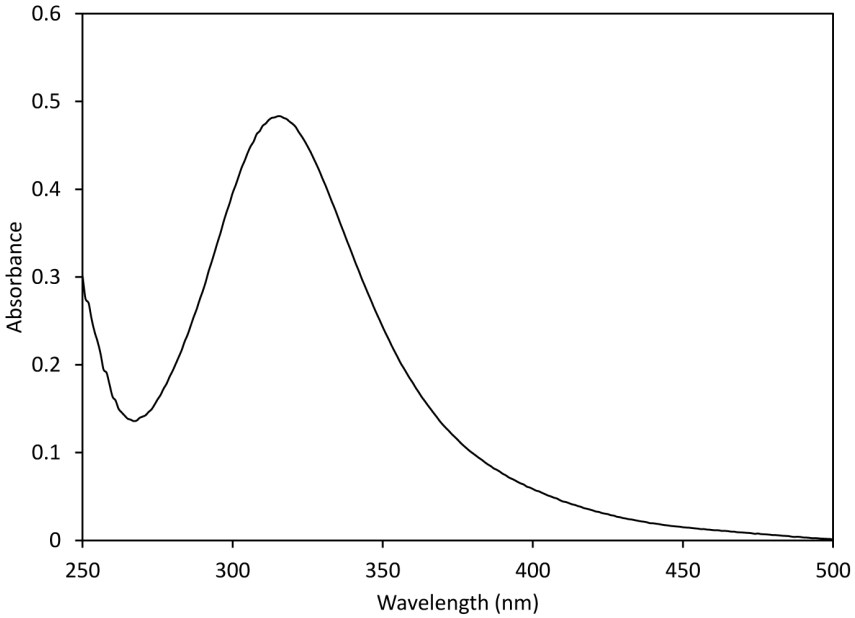

Figure 4. Absorption spectrum of molybdovanadophosphoric acid as obtained in the laboratory.

was designed (Figure 1), where the same micropump was used for standard, sample, and blank solutions. In order to determine which solution was to be dispensed, a so-called gradient manifold, consisting of four solenoid valves (normally closed) with a common port was added (with one of valves left unused).

The timing diagram was redesigned to conform to the new architecture. As an example, the final activation scheme for the measurement of the standard solution is presented in Table 2. The measurement of sample and blank proceed in accordance with similar schemes, optimized to consider the different path lengths.

This system performed satisfactorily, as using the same micropump for standard, sample, and blank solutions ensured that the same volume of each solution was injected into the system.

As to the detection system, it was decided to use as light source an LED emitting in the UV region closer to the wavelength of maximum absorbance around 315 nm (Figure 4).

UV LEDs are still much more expensive than their counterparts for the visible region, those emitting

at shorter wavelengths being considerably more expensive. Also, UV LEDs emitting in the shorter wavelengths exhibit low radiant powers, which in turn affects the signal-to-noise ratio of the measurement. Thus, a wavelength of 365 nm was chosen as a compromise. Based on the ratio of absorbances between this wavelength and the usually employed wavelength of 420 nm, a fourfold gain in sensitivity is to be expected. The LED used in this work features a half-height bandwidth of 12 nm which was deemed sufficiently narrow compared to the absorption band, thus minimizing the risk of nonlinearity of instrumental origin. One drawback of the detection in the UV region is the stray absorption caused by colored samples due to organic matter or other contaminants, which may produce unduly high results. For this reason, the analytical cycle includes as a necessary step the measurement of the sample blank.

Validation

Linearity was studied in preliminary experiments by analyzing a series of 7 standard solutions of orthophosphate containing concentrations up to 6 mg-P L^{-1}. Linearity was satisfactory in this range (R^2 = 0.996). Having ensured this linear range, two-point calibration (blank and a 5 mg-P L^{-1} standard solution) was chosen. The concentration range was consequently restricted to under 5 mg-P L^{-1}.

Precision and accuracy were evaluated in the same experiment by repeatedly analyzing different water samples with phosphorus concentrations in the range 1–5 mg-P L^{-1}. For each sample, analyses were repeated at 6-hour intervals (n = 8). To assess accuracy, additional samples were taken with a lab-made automated sampler at the same times the analyzer was operating and analyzed manually within 24 hours by the APHA reference method [17].

The operating frequency for this experiment (4 day^{-1}) was chosen as a compromise between conditions of repeatability and those prevailing in routine use. Under these conditions precision (s_R (%), n = 8) was in the range of 3%-12% for samples in the 1–5 mg-P L^{-1} range, with better precision corresponding to the more concentrated samples.

As expected, precision was dependent on the phosphorus concentration in the sample. One of the disadvantages of the molybdovanadate method is the high absorbance of the reagent blank. High blank values lead to the subtraction of two similar values which affects precision. It was found that blank values vary with the brand and batch of the ammonium vanadate reagent; thus, some selection of the reagent origin is required to attain better precision.

Also, while the manual reference method employs a rather concentrated reagent, for the automated method it was experimentally determined that with a less concentrated reagent precision was enhanced due to the diminished blank absorbances, while retaining a satisfactory linear range.

For accuracy assessment, an index I = 100 * C_A/C_R was calculated, where C_A stands for the concentration value obtained with the analyzer and C_R is the concentration value obtained with the reference method. Values for I (average for each concentration level, n = 8) ranged from 96.2% to 105.8%. This was deemed fit for the purpose of environmental analysis.

Figure 5 shows the graphical comparison of the results obtained by both methods.

Detection limit (LOD, 3s/m, n = 10) was calculated as 0.061 mg L^{-1}, and quantification limit (LOQ, 10s/m, n = 10) was 0.20 mg L^{-1}.

These figures of merit are better than those obtained in previous work of our group [19, 20], an improvement which we assign to a better-designed flow system and to a higher sensitivity obtained by changing the detection wavelength to one in the UV region.

It is clear that the operating range attained is not adequate for the monitoring of non-polluted water bodies, a decrease of 2 to 3 orders of magnitude in the quantification limit being necessary for this purpose. We are currently addressing our efforts to attain this goal. However, the figures of merit attained in this work are fit for the monitoring of phosphorus levels in polluted water bodies.

Autonomy

System autonomy depends on the charge capacity of the power-bank battery, the electrical consumption of the system, and the volume of stock reagent, standard, carrier (deionized water), and waste bottles. In order to decrease the electrical consumption

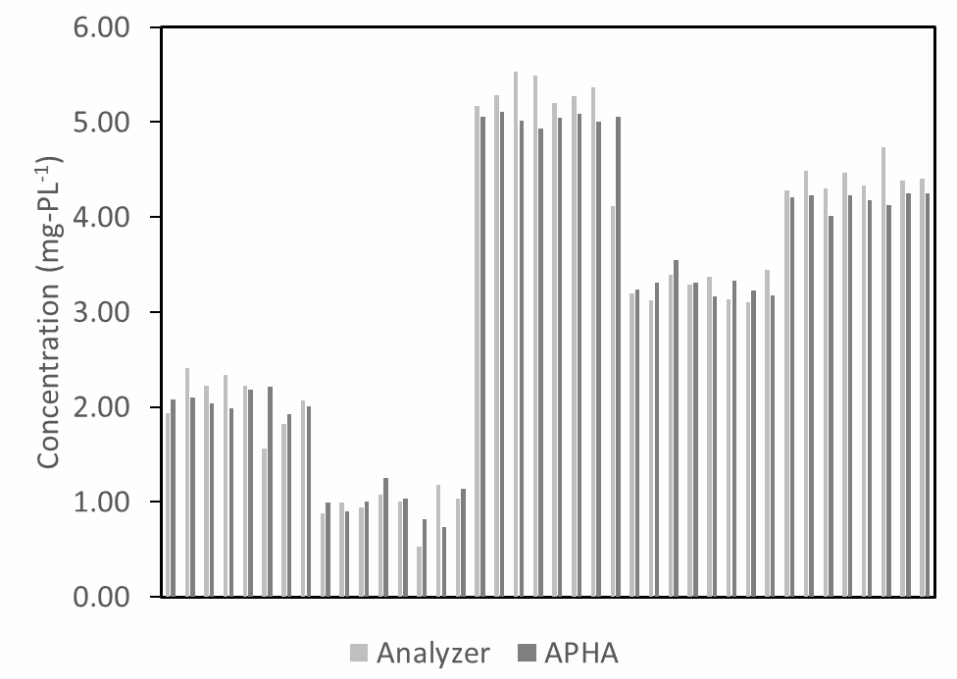

Figure 5. Comparison of results provided by the analyzer (light gray) and the APHA reference method (dark gray) for samples with different phosphorus concentrations.

unnecessary LEDs were avoided in the electronic boards and efficient switching DC-DC step-down converters were used instead of traditional linear regulators. Also, the system was put into a low consumption ("deep sleep") mode between analytical cycles.

Under the operating conditions used in the experiments, an autonomy of one week can be ensured. This can be considered a reasonable period for routine operation, after which the bottles should be replenished, the waste bottle emptied for disposal, and the power bank replaced with a fully charged one.

Applicability of the free cloud-based IoT storage

Currently 2G and 3G technologies are still widely deployed in many countries along with LTE/4G. Thus, the current version of the analyzer uses a low-cost modem, based on the GPRS standard of digital communications. However, considering that GSM and GPRS are being phased out and progressively replaced by LTE/4G and 5G technologies in many regions of the world, the use of a compatible modem should be considered for future versions of the prototype; this, however, does not affect the analyzer itself.

In the present application, communications between the prototype and the Thingspeak server were established by means of a basic protocol addressing the modem with AT commands, and using standard HTTP GET and POST methods for updating the content of the channel. This resulted in satisfactory results albeit at the cost of some messages being lost now and then. Better results could be obtained by using a more robust protocol such as MQTT. This will be included in future versions of the firmware.

Currently there are many IoT servers available, both free and paid, offering different storage capacities and services. The use of cloud-based storage allows not only immediate availability of the results from any location with access to the internet, but also some degree of processing such as data smoothing and plotting right from the platform. The data is also available for download at any time for further processing. In this way, chemical telemetry can be implemented in an easy way.

CONCLUSIONS

The prototype built and evaluated in this work was easy to build, employing mainly off-the-shelf

components and without the need to resort to microfluidics.

In accordance with the goals proposed at the beginning of the project, this design is suitable for self-construction in low budget laboratories.

Performance of the analyzer was satisfactory in terms of the analytical figures of merit, and thus it can be considered fit for the monitoring of the concentrations of phosphorus in polluted water bodies.

ACKNOWLEDGEMENTS

The authors thank Alejandro Schaffner for his skillful assistance with the determinations by means of the reference method.

Moisés Knochen thanks Agencia Nacional de Investigación e Innovación (ANII) for a personal grant.

CONFLICT OF INTEREST STATEMENT

The authors do not have conflicts of interest to declare.

REFERENCES

1. Chorus, I. and Bartram, J. 1999, Toxic Cyanobacteria in Water: A guide to their public health consequences, monitoring and management, E & FN Spon, London - New York.
2. Worsfold, P., McKelvie, I. and Monbet, P. 2016, Anal. Chim. Acta, 918, 8.
3. Miró, M., Estela, J. M. and Cerdà, V. 2003, Talanta, 60, 867.
4. Estela, J. M. and Cerdà, V. 2005, Talanta, 66, 307.
5. Motomizu, S. and Li, Z.-H. 2005, Talanta, 66, 332.
6. Trojanowicz, M. and Pyszynska, M. 2022, Molecules, 27, 1410.
7. Glasgow, H. B., Burkholder, J. A. M., Reed, R. E., Lewitus, A. J. and Kleinman, J. E. 2004, J. Exp. Mar. Biol. Ecol., 300, 409.
8. Mukhopadhyay, S. C. and Mason, A. (Eds.) 2013. Smart sensors for real-time water quality monitoring. Springer-Verlag, Berlin.
9. Nightingale, A. M., Beaton, A. D. and Mowlem, M. C. 2015, Sens. Actuators B Chem., 221, 1398.
10. Lakhwani, K., Gianey, H. K., Wireko, J. K. and Hiran, K. K. 2020, Internet of Things (IoT). Principles, Paradigms and Applications of IoT, PBP Publications, New Delhi.
11. Capella, J. V., Bonastre, A., Campelo, J. C., Ors, R. and Peris, M. 2020, Trends Environ. Anal. Chem., 27, e00095.
12. Garrido-Momparler, V. and Peris, M. 2022, Trends Environ. Anal. Chem., 35, e00173.
13. Murphy, J. and Riley, J .P. 1962, Anal. Chim. Acta, 27, 31.
14. Kitson, R. E. and Mellon, M. G. 1944, Ind. Eng. Chem., Anal. Ed., 16, 379.
15. Abbott, D. C., Emsden, G .E. and Harris, J. R. 1963, Analyst, 88, 814.
16. Nagul, E. A., McKelvie, I. D., Worsfold, P. and Kolev, S. D. 2015, Anal. Chim. Acta, 890, 60.
17. Baird, R. B., Eaton, A. D. and Rice, E. W. (Eds.) 2017, Standard Methods for the Examination of Water and Wastewater, American Public Health Association (APHA), Washington DC, Method 4500-P C.
18. Marczenko, Z. and Balcerzak, Z. 2000, Separation, Preconcentration and Spectrophotometry in Inorganic Analysis, Elsevier, Amsterdam, 328
19. González, P., Pérez, N. and Knochen, M. 2016, Quim. Nova, 39, 305.
20. González, P., Pérez, N. and Knochen, M. 2022, Microchem. J., 175, 107134.
21. Lapa, R. A. S., Lima, J. L. F. C., Reis, B. F., Santos, J. L. M. and Zagatto, E. A. G. 2002, Anal. Chim. Acta, 466, 125.
22. Lima, J. L. F. C., Santos, J. L. M., Dias, A. C. B., Ribeiro, M. F. T. and Zagatto, E. A. G. 2004, Talanta, 64, 1091.
23. González, P., Knochen, M., Sasaki, M. K. and Zagatto, E. A. G. 2015, Talanta, 143, 419.
24. Reis, B.F., Gine, M. F., Zagatto, E. A. G., Lima, J. L. F. C. and Lapa, R. A. 1994, Anal. Chim. Acta, 293, 129.